

Microfabricated Monolithic Multinozzle Emitters for Nanoelectrospray Mass Spectrometry

Woong Kim¹, Mingquan Guo², Peidong Yang^{*l,3} & Daojing Wang^{*2}

1. *The Molecular Foundry and Materials Sciences Division, Lawrence Berkeley*

National Laboratory, Berkeley, California 94720

2. *Life Sciences Division, Lawrence Berkeley National Laboratory, Berkeley,*

California 94720

3. *Department of Chemistry, University of California, Berkeley, California 94720*

Correspondence should be addressed to Daojing Wang djwang@lbl.gov or Peidong

Yang p_yang@uclink.berkeley.edu

Mass spectrometry is the enabling technology for proteomics. To fully realize the enormous potential of lab-on-a-chip in proteomics, major advance in interfacing microfluidics with mass spectrometry is needed. Here, we report the first demonstration of monolithic integration of multinozzle electrospray emitters with a microfluidic channel via a novel silicon microfabrication process. These microfabricated monolithic multinozzle emitters (M^3 emitters) can be readily mass-produced from silicon wafers. Each emitter consists of a parallel silica nozzle array protruding out from a hollow silicon sliver stem with the conduit size of 100×10 μm . The dimension and number of freestanding nozzles can be systematically and precisely controlled during the fabrication process. Once integrated with a mass spectrometer, M^3 emitters achieved sensitivity and stability in peptide and protein detection comparable to those of commercial silica-based capillary nanoelectrospray

tips. These M³ emitters may play a role as a critical component in a fully integrated silicon/silica-based micro total analysis system (TAS) for proteomics.

Mass spectrometry (MS) remains the central tool for proteomics^{1,2}. Technological developments in MS have been a multifaceted and open-ended endeavor. Two current focuses are: 1) continuing improvement in detection sensitivity, resolution, and mass accuracy; and 2) miniaturization of both front-end sample preparation and back-end mass detection. For example, a hybrid linear ion trap/orbitrap mass spectrometer has recently been shown to provide a mass accuracy of up to 2 ppm and a resolving power exceeding 100,000 (FWHM)³. Microfluidic liquid chromatography-mass spectrometry (LC-MS) platforms based on polymer parylene⁴ or polyimide films⁵ have been demonstrated. A handheld rectilinear ion-trap mass spectrometer has recently been built⁶. However, proteome-on-a-chip still remains a challenge due to the lack of technology for high quality interface between microfluidic channels and mass spectrometers⁷.

Despite recent development of new ionization sources such as desorption electrospray ionization (DEI)⁸, matrix-assisted laser desorption ionization (MALDI) and electrospray ionization (ESI) remain the dominant soft-ionization methods for peptides and proteins. Since Fenn et al. first demonstrated the utility of ESI mass spectrometry in analyzing high-molecular-weight biomolecules⁹, extensive scientific and engineering efforts have been made to understand the mechanism of electrospray ionization process and to improve the performance of ESI-MS. One of the most significant steps along this line is the theoretical description and experimental demonstration of nanoelectrospray ionization (nano-ESI)¹⁰ and its applications in protein analysis¹¹. However, the fundamental difference between conventional ESI and nano-ESI has not yet been fully elucidated¹².

Microfabricated monolithic nano-ESI emitters have the potential to contribute to both technological developments and theoretical understanding of nanoelectrospray mass spectrometry. First, they can be mass-produced by microfabrication technology and readily interfaced with microfluidic channels in a lab-on-a-chip proteomic system. Second, they provide a means to systematically alter the size, shape, and density of electrospray nozzles so that fundamental mechanisms underlying the electrospray ionization process can be studied. There have been efforts to fabricate ESI emitters using either polymeric materials or silicon-based materials. The former includes nozzles made of parylene^{13,14}, poly(dimethylsiloxane) (PDMS)¹⁵, poly(methylmethacrylate) (PMMA)¹⁶, and a negative photoresist, SU-8^{17,18}. The latter includes nozzles made of silicon nitride using in-plane fabrication¹⁹ and of silicon/silica using out-of-plane processes^{20,21}. However, hydrophobic polymers have inherently undesirable properties for the electrospray application, such as strong affinity to proteins and incompatibility with certain organic solvents^{22,23}. In-plane fabrication was not pursued further apparently due to the intrinsic clogging problem arising from the etching of sacrificing layer of phosphosilicate glass between two layers of silicon nitride¹⁹. Out-of-plane fabrication is critically limited in terms of the flexibility to produce monolithically integrated built-in structures and requires additional assembly steps to attach nozzles to the end of a microfluidic channel. More recent efforts to generate nanoelectrospray from nanofluidic capillary slot²⁴ and micromachined ultrasonic ejector array²⁵ faced similar challenges.

Here, we report a novel silicon/silica-based microfabrication process that is straightforward and flexible for the monolithic fabrication of biocompatible M³ emitters. Our fabrication process requires only one mask and consists of five major steps (**Fig. 1**).

A photolithographic patterning step defines the size and the shape of the microfluidic channels (**Fig. 1a**). Deep reactive ion etching combined with silicon fusion bonding encloses the microfluidic channels (**Fig. 1b,c**). Oxidation and XeF₂ etching generates protruding nanoelectrospray nozzles made of SiO₂ (**Fig. 1d,e**). The process is significantly simplified compared to the previous examples¹⁹⁻²¹ and generates biocompatible monolithic microfluidic channels connected with multinozzles. A distinctive advantage of our process is its versatility and its amenability for large-scale production. The nanoelectrospray emitters with various size and number of protruding nozzles were monolithically fabricated with unprecedently high array density (line density = 100 nozzles/mm).

EXPERIMENTAL SECTION

Microfabrication of nanoelectrospray emitters. A layout of microfluidic channels (~ 6 cm long) were photolithographically patterned on a (100) p-type silicon wafer of 4-inch diameter ($\rho = 15 \sim 30 \Omega \text{ cm}$). After the development of the exposed photoresist, the area for the channels was etched down via deep reactive ion etching (DRIE) process using the advanced silicon etching (ASE) system of surface technology systems (STS). The depths of the channels were measured using a surface profiler. After the removal of the photoresist, the wafer was cleaned in piranha solution at 120 °C and thoroughly rinsed with deionized (DI) water (~ 18 MΩ) and spun dry. Immediately after the cleaning and drying step, the patterned wafer was gently pressed with a clean plane wafer under a sink equipped with high efficiency particulate air (HEPA) filters. These pre-bonded wafer

pair were then annealed in the stream of N₂ flow at 1050 °C for 1 hour for silicon-silicon fusion bonding, which generates covalent bonding between the two wafers.

After the aforementioned channel etching and the wafer bonding steps, the microfluidic channels were enclosed inside the bonded wafer. To open up each side of the channels, both sides of the wafer were cut using an automatic wafer saw. After that, SiO₂ was thermally grown on the wafer including the surface of the open channel inside the wafer. The wet oxidation process at 1050 °C for 10 hours yielded the oxide with a thickness of ~ 1.9 μm. Around 2 ~ 3 mm of nozzle side of the wafer were cut off to remove SiO₂ capping layer and expose silicon at this end of the wafer. After the wafer was cut into individual electrospray tips, the exposed silicon at the ends of the tips was selectively etched away against SiO₂ using XeF₂ as the etching gas. This selective silicon etching step leaves behind protruding nozzles made of SiO₂ (length ~ 200 μm). The tips went through 200 to 250 cycles of XeF₂ etching and N₂ purging. Each etching step was carried out for 60 seconds under the pressure of 4 torr of XeF₂ and 2 torr of N₂.

Connection of the spray emitters. An analyte solution was infused through a 500 μl syringe. A syringe pump was used to maintain the constant flow rate. A capillary tube (i.d. ~ 75 μm) from the syringe was connected to the fabricated electrospray emitters via Teflon tubes. Epoxy adhesive was applied to seal the connection and cured overnight at room temperature before use.

Nanoelectrospray mass spectrometry. Glu-Fibrinopeptide B (GFP B) was purchased from Sigma and dissolved in a solvent of 30 % acetonitrile and 0.1% formic acid in deionized water. Bovine serum albumin and Myoglobin are purchased from Amersham biosciences and Sigma, respectively, and prepared in the same way as the

GFP B solution. All analyte solutions were at 1 M concentration. All electrospray ionization mass spectrometry experiments were performed on a Q-TOF API US mass spectrometer of Waters Corp. The instrument was calibrated and optimized with standard compounds as suggested by the manufacturer. Except for the electrospray voltages applied, identical instrument conditions were utilized for fabricated emitters and commercial tips during the comparison.

Results and Discussion

Microfabrication of M³ Emitters. We have incorporated Micro-Electro-Mechanical System (MEMS) techniques in the fabrication process. For example, the channels were etched and enclosed between two wafers by the combination of deep reactive ion etching and silicon fusion bonding techniques. This combination is a versatile tool and has been demonstrated to fabricate various micromechanical devices²⁶. In the etching step, silicon channels are etched down via time-multiplexed SF₆ etching and C₄F₈ passivation cycles²⁷. In the bonding step, two piranha cleaned wafers are first held together via hydrogen bonding between the silanol groups of the surfaces of each wafer. Subsequent high temperature annealing of the pre-bonded wafers enables the formation of the Si-O-Si covalent bonds at the interface of the wafers. The bond strength of these wafers is on the order of the yield strength of single-crystal silicon (~ 1 GPa)²⁸. This feature makes our microfluidic structures practically monolithic and imparts high bonding quality against leakage and rupture. No physical gap at the interface was observed under scanning electron microscopy (SEM) and no fluid leakage was detected during the operation of electrospray mass spectrometry. Since hydrophilicity of the channel was very important

for the capillary action to occur, all channels were treated with piranha solution before use. Owing to the hydrophilic properties of SiO_2 , our electrospray emitters are intrinsically more compatible with various biomolecules than hydrophobic polymer based electrospray emitters.

SEM was used to examine the microfabricated structures (**Figure 2b-g**). A schematic view of the M^3 emitters is shown in **Figure 2a**. The final product is a bonded chip of silicon sliver stem with an embedded microfluidic channel that is 100- μm wide and 10- μm deep, and monolithically integrated silica multinozzles. The nozzles protrude about 150 to 250 μm from the end of silicon stem. These protruding nozzles are made of SiO_2 and are the result of the selective etching of surrounding Si by XeF_2 . The selectivity of Si etching against SiO_2 was roughly 400 to 1. The oxide thickness of the nozzle tips was $\sim 1 \mu\text{m}$ after the etching step.

Our process is straightforward but not limited in fabricating complicated structures. For example, multiple nozzles were fabricated at the end of electrospray emitters (**Fig. 2d-g**). **Figure 2e,f** show five 10 $\mu\text{m} \times 12 \mu\text{m}$ ($W \times D$) nozzles branching out of the main channel which has a cross sectional area that is 100- μm wide and 12- μm deep. Inter-nozzle space in this case is about 10 μm . **Figure 2g** shows an array of ten protruding nozzles (2 $\mu\text{m} \times 8 \mu\text{m}$) in the cross sectional area of 100 $\mu\text{m} \times 8 \mu\text{m}$ of a main channel. It approximately corresponds to an area density of $\sim 10^4$ nozzles/ mm^2 and linear density of 100 nozzles/ mm . This is an unprecedentedly high nozzle density. For comparison, a nozzle array with density of 2.5 nozzles/ mm^2 was recently fabricated via out-of-plane approach²⁹. Using the same process and by only changing the layout, complex built-in structures can be monolithically fabricated at the main channel side as well⁵. With further

optimization, it is also possible to fabricate M³ emitters down to submicron in nozzle size and up to 10⁶ nozzles/mm² in density. A total of 55 emitters with various numbers and sizes of the nozzles were fabricated on a bonded wafer, and this number can be easily increased by several factors by optimizing the dimensions and layout of the emitters.

Nanoelectrospray Mass Spectrometry using M³ Emitters. We first tested the viability of these novel M³ emitters using organic solvents. The solvents were delivered to the inlet of the sliver stem that had a rectangular opening of 100- m width and 10- m depth (**Figure 2a**). The solution then passed through the slab-like hollow channel and sprayed off from the nozzles (10 m × 10 m) at the other side of the stem. The length, width, and height of the whole chip were approximately 5.5 cm, 600 m, and 1 mm, respectively. These dimensions were made similar to those of pulled-out capillary nanoelectrospray tips (purchased from New Objective, Inc.) used for comparison in this study (length ~ 7.5 cm, outer diameter of the capillary ~ 360 m, and inner diameter of orifice ~ 10 m). We observed that the protrusion of the nozzles was critical for generating electrospray ionization. It isolated initial liquid droplets at the tips of nozzles from the surface of the silicon stem and prevented the droplets from wetting the surface. When the length of the nozzles was below tens of microns, no electrospray was observed due to the wetting problem, similar to the case of flat edge tips. The difficulty of the electrospray generation from flat edge tips due to the surface tension was reported previously³⁰.

We then tested the performance of the M³ emitters for potential proteomic applications. We used M³ emitters containing a single nozzle (10 m × 8 m) and did a head-to-head comparison with commercially available, pulled fused-silica capillary

nanoelectrospray tips with an orifice inner diameter of \sim 10 μm (SilicaTipsTM, New Objective, Inc). The M³ emitters were integrated with a Q-TOF mass spectrometer (Waters Inc.). Since the emitters were made of conductive silicon, they were used without additional metal coatings. In contrast, most of the commercial silica-based ESI tips need to be coated with Pt or Au. First, a standard peptide, [Glu¹]-Fibrinopeptide B (GFP B, M.W. = 1570.57) was tested. The GFP B solution (1 M) was delivered to the nozzle at a flow rate of 600 nl/min, as described in the method section. **Figure 3a** and **b** show the mass spectra obtained from the fabricated emitter and the commercial tip, respectively. The isotopic distributions of doubly-charged ions of GFP B were clearly observed and similar magnitudes of base peak intensity (BPI) of about 1,000 per scan were obtained in both cases. This indicates that the resolution and the sensitivity of our fabricated emitters are comparable to those of commercial tips. However, higher voltage (4.5 kV \sim 4.8 kV) was needed for the fabricated emitters than for the commercial tips (2.1 kV \sim 2.4 kV). We conjecture that depositing metal on the tips or using more conductive silicon wafers may lower the required voltage. Since we were using a platform that was already optimized for the commercial tips, detailed optimization on any electrical and mechanical connections of the fabricated emitters may lower the voltage as well.

Since detecting masses of full length proteins is equally important as detecting those of proteolytic peptides in proteomics, we further compared the performance of our M³ emitters with commercial tips for detecting high molecular weight proteins. Similar results were obtained as shown in the mass spectra of bovine serum albumin (BSA, \sim 67 kDa) that were accumulated for 10 min (**Fig. 4a,b**). Charge state distribution and base peak intensity were similar in both cases. They showed 38 or more charge states of the

protein with the highest peak at around 1,340, which corresponds to about 50 positive charges. **Figure 4c,d** show that the stability of our emitters (relative standard deviation, RSD ~ 4.5 %) is comparable to that of commercial tip (RSD ~ 4.2 %).

Finally, our unique microfabrication process enables direct performance comparison between a multinozzle emitter (10 μm × 12 μm) and a single-nozzle emitter (10 μm × 12 μm). Since the flow rate at the silicon sliver stem was kept constant at 600 nl/min, the flow rate at each nozzle on average was 120 nl/min for the 5-nozzle emitter. Mass spectra of myoglobin (~17 kD) obtained from a single- and a five-nozzle emitters are shown in **Figure 5a,b**. Electrospray was observed from each of the five nozzles. However, two outer nozzles generated bigger droplets similarly to those observed and described in a large scale multinozzle spray previously²⁹. In general, multinozzle emitters showed similar performance yet slightly higher sensitivity than that of the single nozzle emitters. Multinozzle emitters are expected to ease back pressure and clogging problem that single nozzle emitters have to cope with, especially as the channel downsizes to submicron scale. In addition, high-density multinozzle emitters provide a valuable means to study ionization process since extremely low flow rate can be achieved at each single nozzle.

CONCLUSIONS

In summary, we presented a novel and significantly simplified procedure for the microfabrication of fully integrated nanoelectrospray emitters. It consists of an etching and silicon fusion bonding step for the formation of enclosed channel, and an oxidation and XeF₂ etching step for the formation of protruding multinozzles. These microfabricated monolithic multinozzle emitters (M^3 emitters) showed comparable

performance to that of the commercial tips in terms of stability and sensitivity for a standard peptide and high molecular weight proteins. With further device optimization, additional performance enhancement is expected. Our process is straightforward, yet fully capable of producing complicated structures such as high density array of overhanging nozzles that are monolithically integrated with a microfluidic channel. The simplicity and the versatility of our process may be potentially utilized to fabricate other complex bio-analytical tools.

Acknowledgements

This work was supported by National Institutes of Health Grant GM077870 (to D.W.). Part of this work was performed at the Molecular Foundry, Lawrence Berkeley National Laboratory, which is supported by the Office of Science, Office of Basic Energy Sciences, of the U.S. Department of Energy under Contract No. DE-AC02-05CH11231.

References

- (1) Aebersold, R.; Mann, M. *Nature* **2003**, *422*, 198-207.
- (2) Domon, B.; Aebersold, R. *Science* **2006**, *312*, 212-217.
- (3) Makarov, A.; Denisov, E.; Kholomeev, A.; Baischun, W.; Lange, O.; Strupat, K.; Horning, S. *Anal. Chem.* **2006**, *78*, 2113-2120.
- (4) Xie, J.; Miao, Y. N.; Shih, J.; Tai, Y. C.; Lee, T. D. *Anal. Chem.* **2005**, *77*, 6947-6953.
- (5) Yin, N. F.; Killeen, K.; Brennen, R.; Sobek, D.; Werlich, M.; van de Goor, T. V. *Anal. Chem.* **2005**, *77*, 527-533.
- (6) Gao, L.; Song, Q. Y.; Patterson, G. E.; Cooks, R. G.; Ouyang, Z. *Anal. Chem.* **2006**, *78*, 5994-6002.
- (7) Freire, S. L. S.; Wheeler, A. R. *Lab Chip* **2006**, *6*, 1415-1423.
- (8) Takats, Z.; Wiseman, J. M.; Gologan, B.; Cooks, R. G. *Science* **2004**, *306*, 471-473.
- (9) Fenn, J. B.; Mann, M.; Meng, C. K.; Wong, S. F.; Whitehouse, C. M. *Science* **1989**, *246*, 64-71.
- (10) Wilm, M. S.; Mann, M. *Int. J. Mass Spectrom. Ion Processes* **1994**, *136*, 167-180.
- (11) Wilm, M.; Shevchenko, A.; Houthaeve, T.; Breit, S.; Schweigerer, L.; Fotsis, T.; Mann, M. *Nature* **1996**, *379*, 466-469.
- (12) Juraschek, R.; Dulcks, T.; Karas, M. *J. Am. Soc. Mass Spectrom.* **1999**, *10*, 300-308.
- (13) Licklider, L.; Wang, X. Q.; Desai, A.; Tai, Y. C.; Lee, T. D. *Anal. Chem.* **2000**, *72*, 367-375.

- (14) Yang, Y. N.; Kameoka, J.; Wachs, T.; Henion, J. D.; Craighead, H. G. *Anal. Chem.* **2004**, *76*, 2568-2574.
- (15) Kim, J. S.; Knapp, D. R. *J. Am. Soc. Mass Spectrom.* **2001**, *12*, 463-469.
- (16) Schilling, M.; Nigge, W.; Rudzinski, A.; Neyer, A.; Hergenroder, R. *Lab Chip* **2004**, *4*, 220-224.
- (17) Le Gac, S.; Arscott, S.; Rolando, C. *Electrophoresis* **2003**, *24*, 3640-3647.
- (18) Nordstrom, M.; Marie, R.; Calleja, M.; Boisen, A. *J. Micromech. Microeng.* **2004**, *14*, 1614-1617.
- (19) Desai, A.; Tai, Y.; Davis, M. T.; Lee, T. D. International Conference on Solid State Sensors and Actuators (Transducers '97), Piscataway, NJ, **1997**, 927-930.
- (20) Schultz, G. A.; Corso, T. N.; Prosser, S. J.; Zhang, S. *Anal. Chem.* **2000**, *72*, 4058-4063.
- (21) Griss, P.; Melin, J.; Sjodahl, J.; Roeraade, J.; Stemme, G. *J. Micromech. Microeng.* **2002**, *12*, 682-687.
- (22) Huang, B.; Wu, H. K.; Kim, S.; Zare, R. N. *Lab Chip* **2005**, *5*, 1005-1007.
- (23) Lee, J. N.; Park, C.; Whitesides, G. M. *Anal. Chem.* **2003**, *75*, 6544-6554.
- (24) Arscott, S.; Troadec, D. *Appl. Phys. Lett.* **2005**, *87*.
- (25) Aderogba, S.; Meacham, J. M.; Degertekin, F. L.; Fedorov, A. G.; Fernandez, F. M. *Appl. Phys. Lett.* **2005**, *86*.
- (26) Klaassen, E. H.; Petersen, K.; Noworolski, J. M.; Logan, J.; Maluf, N. I.; Brown, J.; Stormont, C.; McCulley, W.; Kovacs, G. T. A. *Sens. Actuators, A* **1996**, *52*, 132-139.

- (27) Blaw, M. A.; Zijlstra, T.; van der Drift, E. *J. Vac. Sci. Technol., B* **2001**, *19*, 2930-2934.
- (28) Barth, P. W. *Sens. Actuators, A* **1990**, *23*, 919-926.
- (29) Deng, W. W.; Klemic, J. F.; Li, X. H.; Reed, M. A.; Gomez, A. *J. Aerosol Sci.* **2006**, *37*, 696-714.
- (30) Xue, Q. F.; Foret, F.; Dunayevskiy, Y. M.; Zavracky, P. M.; McGruer, N. E.; Karger, B. L. *Anal. Chem.* **1997**, *69*, 426-430.

Figure Captions

Figure 1. Microfabrication process of multinozzle nanoelectrospray emitters a) photolithographic patterning of microfluidic channels, b) development of photoresist and deep reactive ion etching of the channels, c) silicon fusion bonding with a plane wafer and opening the channels on both side of the wafer, d) thermal oxidation and water cutting to expose silicon on nozzle side, and e) selective silicon etching against SiO_2 by XeF_2 .

Figure 2. a) A schematic view of a nanoelectrospray emitter with two protruding nozzles. $L = 5.5 \text{ cm}$, $W = 0.6 \text{ mm}$, $H = 1\text{mm}$. The length of the protruding part of the nozzles is $\sim 200 \text{ }\mu\text{m}$ (not to scale). b) Scanning electron microscopy (SEM) image of a protruding single-nozzle spray emitter. c) A magnified image of the nozzle that is $10\text{- }\mu\text{m}$ wide and $12\text{- }\mu\text{m}$ deep. d) A double-nozzle emitter ($10 \times 12 \text{ }\mu\text{m}$). e) A five-nozzle emitter. f) Zoom-in image of e) ($10 \times 12 \text{ }\mu\text{m}$ nozzle). g) A ten-nozzle emitter ($2 \text{ }\mu\text{m}$ wide and $8 \text{ }\mu\text{m}$ deep nozzle).

Figure 3. Mass spectra of 1 M GFP B obtained from a) a single-nozzle emitter ($10 \text{ }\mu\text{m} \times 8 \text{ }\mu\text{m}$) and b) a commercial capillary tip (i.d. $\sim 10 \text{ }\mu\text{m}$). 4.5 kV and 2.1 kV were applied to the fabricated emitters and the commercial tips, respectively. The flow rate was 0.6 l/min for all tips.

Figure 4. Mass spectra of 1 M BSA obtained from a) a single-nozzle emitter and b) a commercial tip. Total ion counts of 1 M BSA over time obtained from c) the single-nozzle emitter and d) the commercial tip.

Figure 5. Mass spectra of 1 M myoglobin obtained from a) a single-nozzle emitter and b) a five-nozzle emitter.

Figure 1.

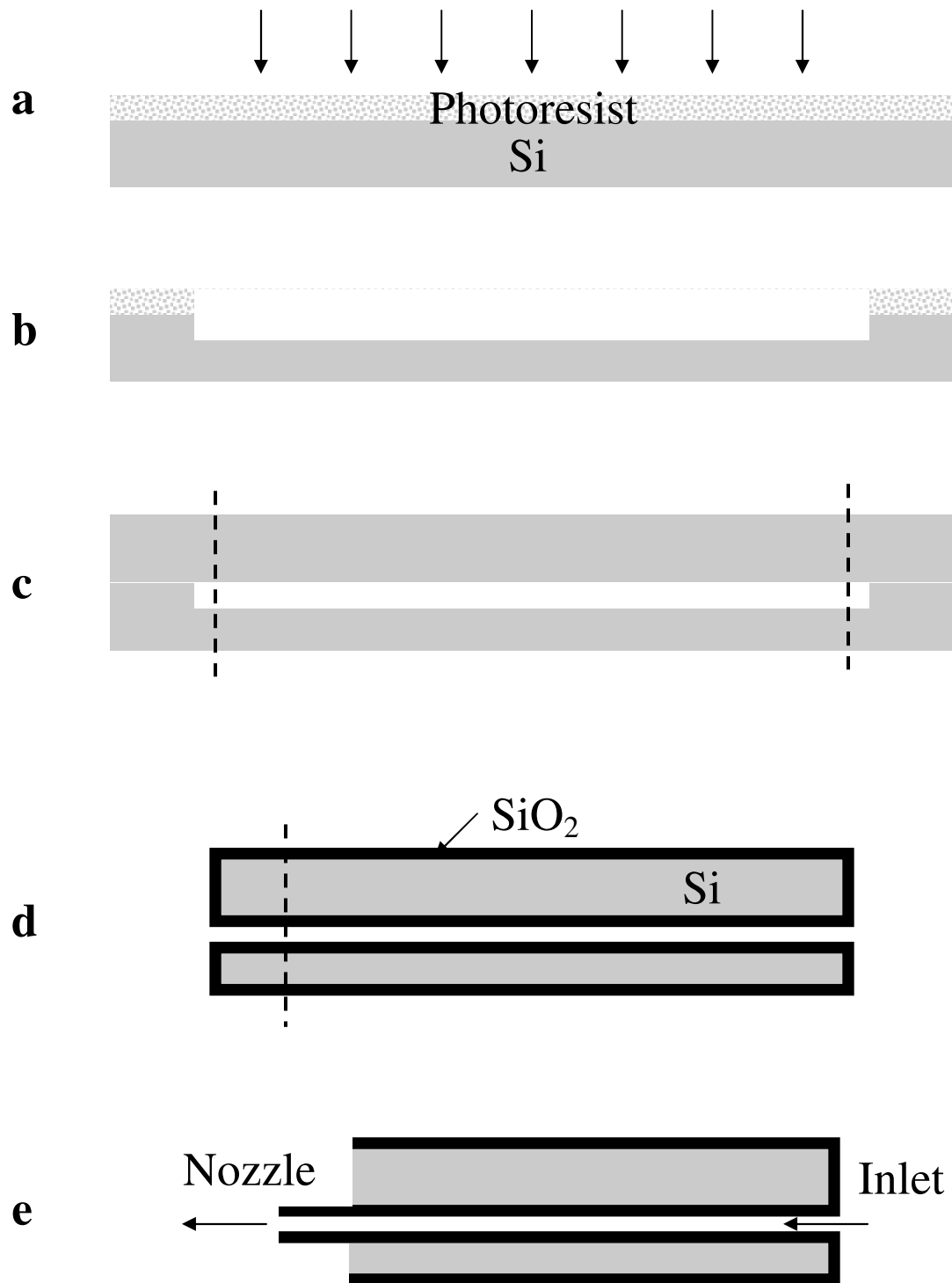


Figure 2.

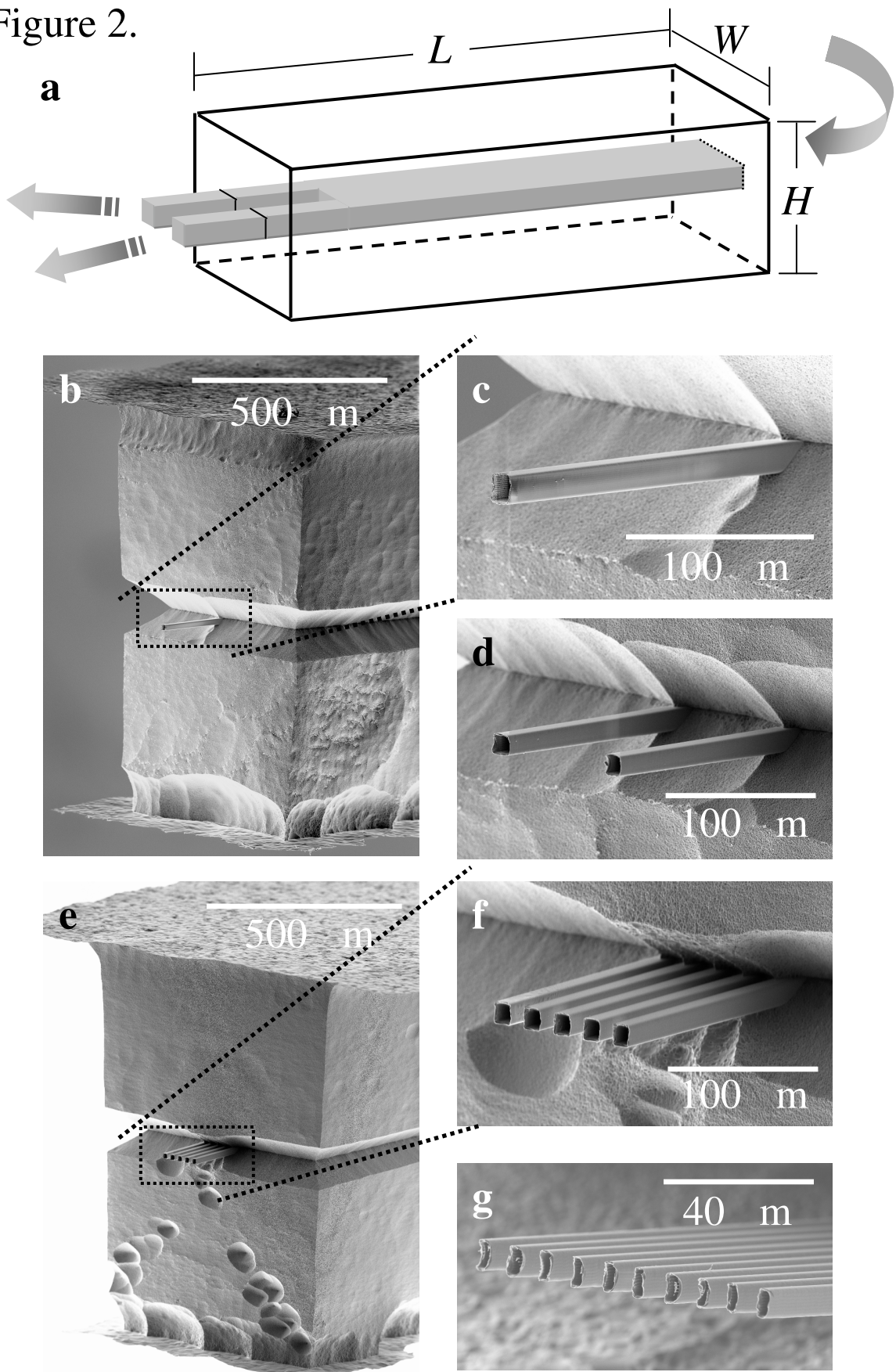


Figure 3.

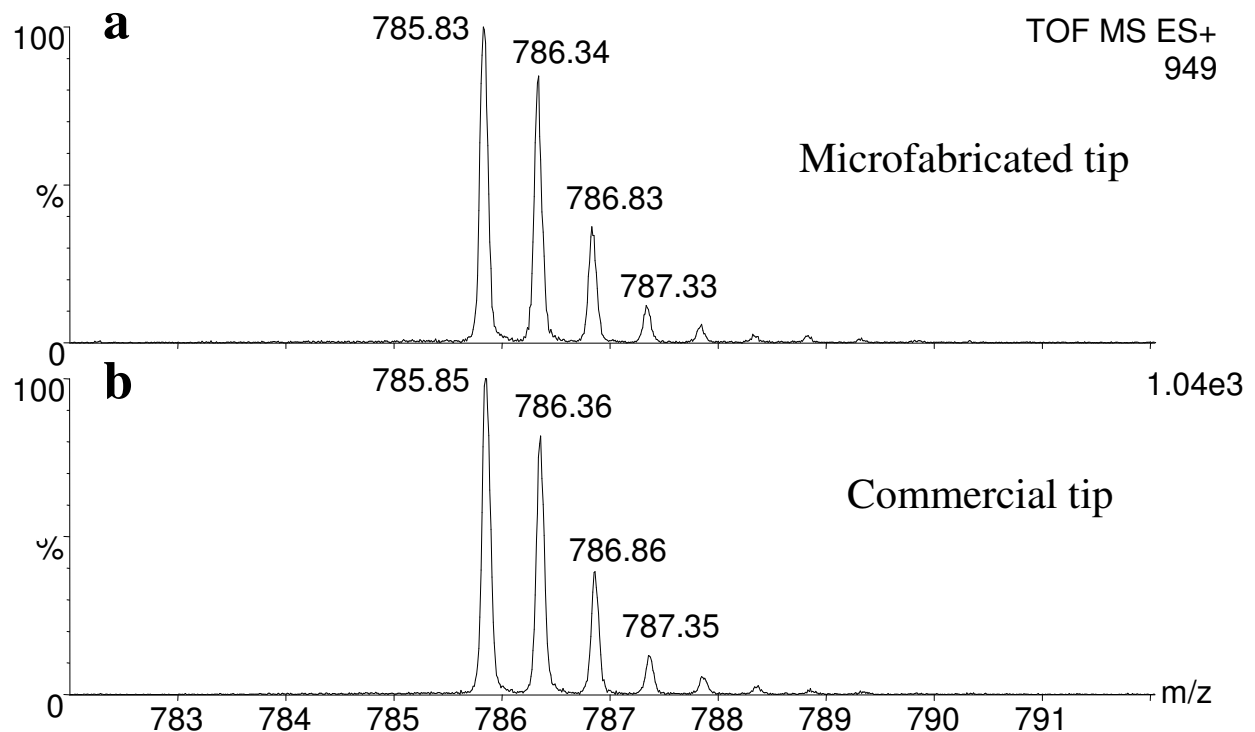


Figure 4.

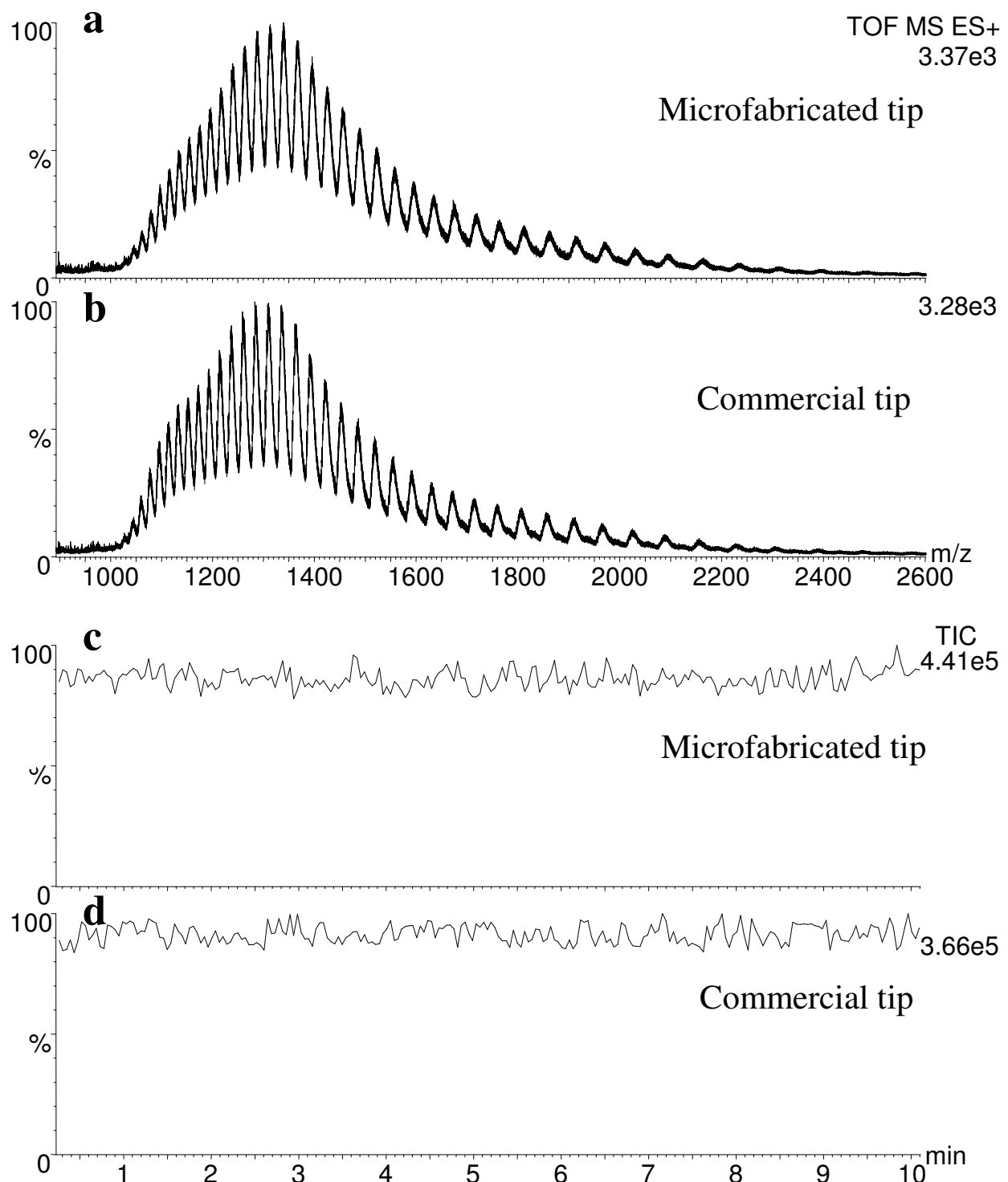


Figure 5.

